

Development of folate functionalized bioactive glass nanoparticles for drug-free nanotherapy of inflamed tissues

Xiang-Ting Fu^{1,2,4,5}, Yu-Meng Li^{1,2,4,5}, Jung-Hwan Lee^{1,2,3,4,5}, Hae-Hyung Lee^{1,2,3,4,5*}, Hae-Won Kim^{1,2,3,4,5*}

¹Institute of Tissue Regeneration Engineering (ITREN), Dankook University, Cheonan 31116, Republic of Korea

²Department of Nanobiomedical Science and BK21 PLUS NBM Global Research Center for Regenerative Medicine, Dankook University, Cheonan 31116, Republic of Korea

³Department of Biomaterials Science, College of Dentistry, Dankook University, Cheonan 31116, Republic of Korea

⁴UCL Eastman-Korea Dental Medicine Innovation Centre, Dankook University, Cheonan 31116, Republic of Korea

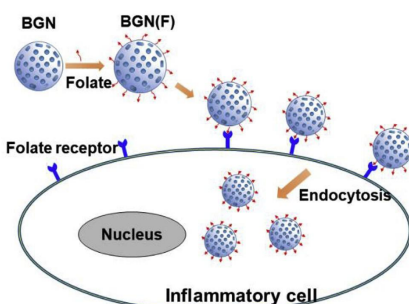
⁵Cell & Matter Institute, Dankook University, Cheonan 31116, Republic of Korea

*Correspondence: healee@dku.edu / kimhw@dku.edu

Introduction

Bioactive glass nanoparticles (BGNs), have recently gained special interest, due to their unique potential as nanocarriers of therapeutic molecules and nanocomponents in bioactive composites for cell scaffolds. There were few reports about the regenerative potential of BGNs and biological actions in inflammatory/immune response. Here, we functionalized the surface of BGN with folate (named BGN(F)) to target pro-inflammatory cells and investigate the anti-inflammatory effects of the BGN(F) on the pro-inflammatory cells, and the possible molecular mechanisms underlying the events.

Materials & Methods



Schematic illustration showing the interaction of BGN(F) with a targeted inflammatory activated cell.

- BGNs, with a Si/Ca ratio of 85/15, were first aminated with (3-aminopropyl) triethoxysilane (APTES) and then functionalized with folate (folic acid).
- The characterizations of particles were observed by TEM and ATR-FTIR.
- The release of silicate and calcium ions was monitored by ICP-AES.
- The changes in gene and protein levels of inflammatory cells were detected by RT-PCR, ELISA kit, Immunocytochemistry and FACS.
- Histological and immunohistochemical staining were performed to evaluate the anti-inflammatory effects in vivo.

Results & Discussion

Fig.1. Characteristics of functionalized nanoparticles

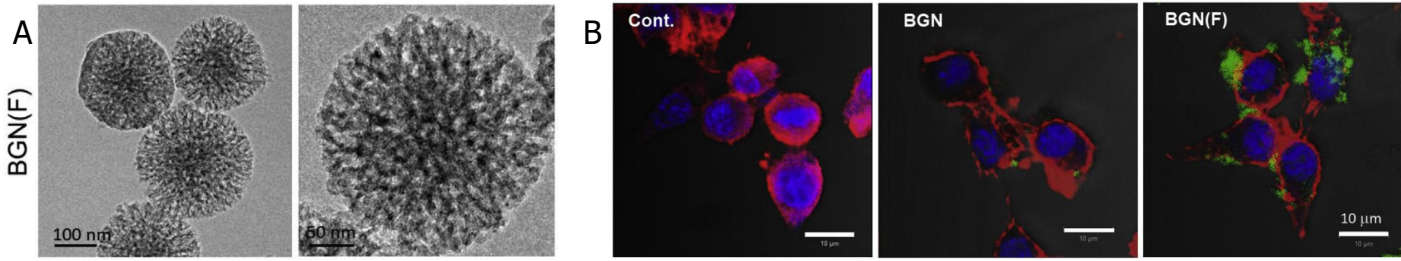


Fig.1.(A) TEM images showing folate-conjugated BGN (BGN(F)) with uniform size and highly mesoporous structure.

Fig.1.(B) Confocal microscopic images of cells (cultured in normal medium) representatively shown with the treatment of nanoparticles.

Fig.2. Expression of inflammation related genes

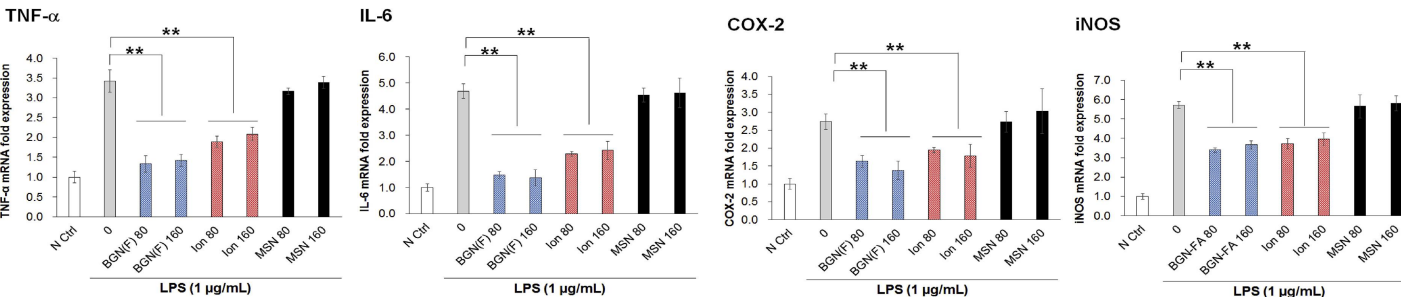


Fig.2. Treatment of BGN(F) 80 or 160 to LPS-induced RAW 264.7 cells for 24 h significantly reducing the expression of inflammation related genes (TNF-α, IL-6, COX-2 and iNOS), as analyzed quantitatively by qRT-PCR. Effects of MSN and the ionic extracts (Ion) of BGN(F) on cells also examined for comparison purpose. Statistical significant difference noticed between groups (**P < 0.01).

Fig.3. Cellular expression of inflammation-related proteins

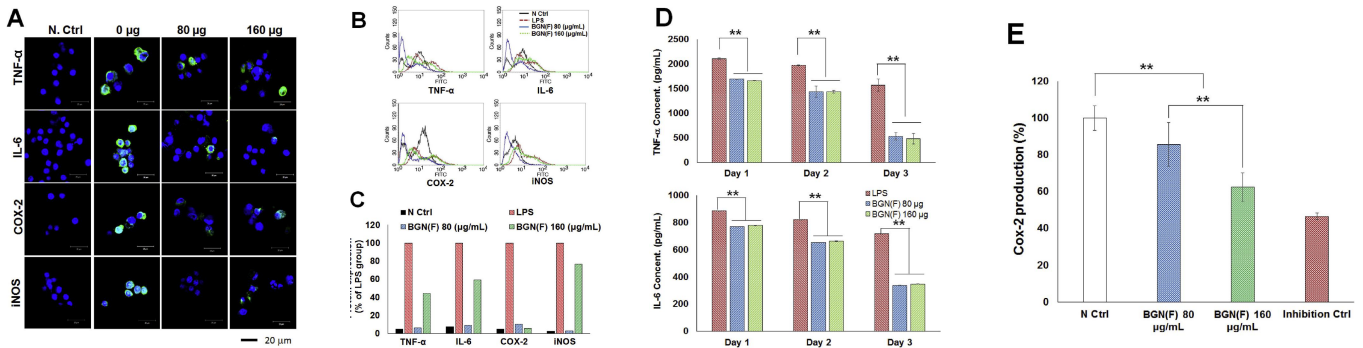


Fig.3. (A) Immunocytochemical staining of cells, Inflammatory related proteins exhibit green signals. Cells counter stained with DAPI (blue); (B, C) FACS assay; representative histograms (B) and bar graphs quantified (C); (D) Release of inflammatory cytokines from cells, as monitored by ELISA; (E) COX-2 inhibition assay analyzed by COX-2 Inhibitor Screening Kit.

Fig.4. Polarization of macrophages

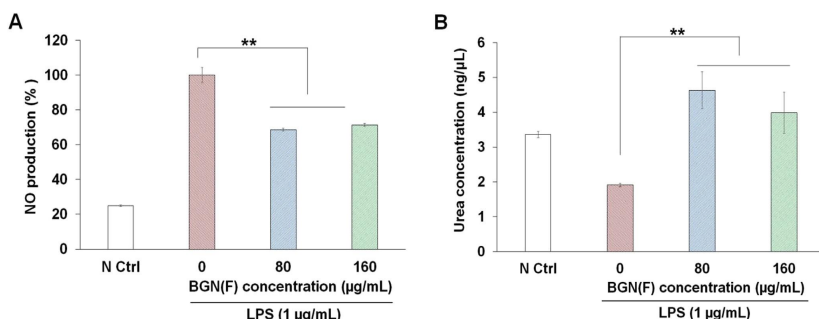


Fig.4. Macrophage polarization by BGN(F) in LPS-stimulated RAW 264.7 cells, analyzed by the production of (A) nitric oxide (NO) for M1 and (B) urea for M2. Significant difference noticed between groups (**P < 0.01).

Results & Discussion

Fig.5. In vivo efficacy of BGN(F)

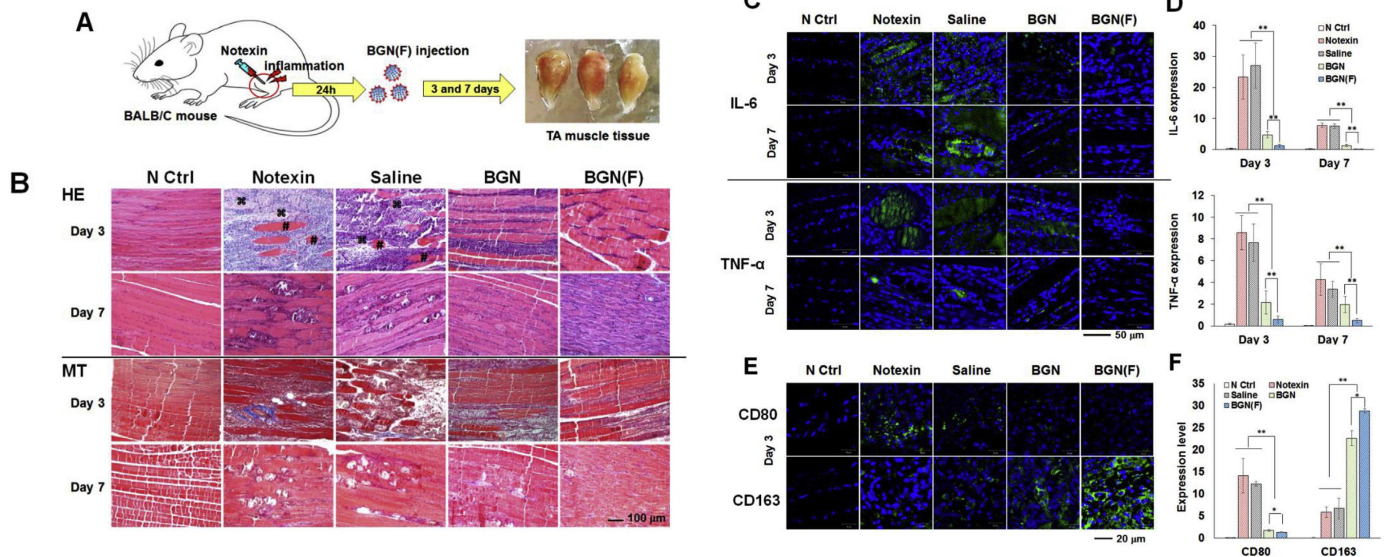


Fig.5. (A) Schematic illustration of mouse tibialis anterior (TA) muscle injury model. (B) Representative histological images. TA muscle tissues without any treatment used as a negative control (N Ctrl), and those treated with Notexin (Notexin) or Notexin-then-saline (Saline) used as positive controls (n = 5). Notexin or Saline groups induced myofiber necrosis (#) and degeneration (*) and recruited a number of inflammatory cells. (C, D) Immunohistochemical analysis of the IL-6 and TNF- α in tissue samples. Revealing green(+) signals of IL-6 and TNF- α (nucleus counterstained with DAPI in blue) (C), and the expressions quantified from the fluorescence intensity (**P < 0.01) (D). (E, F) Polarization of macrophages in the tissue samples. Revealing classically activated (M1) macrophages positive for CD80 and alternatively activated (M2) macrophages for CD163 (in green) (E), and the expressions of markers quantified from the fluorescence intensity (F) (*P < 0.05, **P < 0.01).

Summary & Conclusions

The treatment of BGN(F) at proper concentrations rescued the LPS-induced inflammatory cell viability with reduced cell death, LDH release and ROS generation, down-regulated the expression of pro-inflammatory through the suppression of phosphorylation of the molecules involved in the intracellular signaling and showed the potential to switch the macrophage polarization from pro-inflammatory M1 to anti-inflammatory M2 status. This study shows that drug-free synthetic nanoparticles BGN(F) that target and internalize proinflammatory cells and release ions, ultimately demonstrating profound anti-inflammatory functions in vitro and in vivo support their uses as novel drug-free nanotherapeutic platform for the treatment of inflamed tissues.

References

1. T.H. Kim, et al. Anti-inflammatory actions of folate-functionalized bioactive ion-releasing nanoparticles imply drug-free nanotherapy of inflamed tissues, *Biomaterials*, 207 (2019), pp. 23-38
2. H.Y, et al. Inhibition of lanthanide nanocrystal-induced inflammasome activation in macrophages by a surface coating peptide through abrogation of ROS production and TRPM2-mediated Ca²⁺ influx, *Biomaterials*, 108 (2016), pp. 143-156
3. D. H. et al. Shifts in macrophage phenotype at the biomaterial interface via IL-4 eluting coatings are associated with improved implant integration, *Biomaterials*, 112 (2017), pp. 98-107

Acknowledgement

This work was supported by a National Research Foundation of Korea (NRF) grant funded by the Global Research Development Center Program (2018K1A4A3A01064257) and by the Priority Research Center Program provided by the Ministry of Education (2019R1A6A1A11034536).